

Defect versus defect: stationary states of single file marching in periodic landscapes with road blocks

Atri Goswami,^{1,2,*} Rohn Chatterjee,^{2,†} and Sudip Mukherjee^{2,‡}

¹*Gurudas College, 1/1, Suren Sarkar Road, Jewish Graveyard,
Phool Bagan, Narkeldanga, Kolkata 700054, West Bengal, India*

²*Barasat Government College, 10, KNC Road, Gupta Colony, Barasat, Kolkata 700124, West Bengal, India*

(Dated: April 23, 2024)

Totally asymmetric simple exclusion process (TASEP) sets the paradigm for one-dimensional driven single file motion. We study a periodic TASEP with two “road blocks” or defects of different kinds, one point and another extended, across which particle flows are inhibited. We show how the interplay between particle number conservation and competition between the defects lead to inhomogeneous steady states with localised domain walls (LDW) or static density shocks, whose locations jump discontinuously, indicating a first order transition between these LDW states, as the system passes from being controlled by one defect to the other. When the defects are “competing”, instead of an LDW a pair of delocalised domain walls are found, none of which can penetrate the extended defect. A minimum current principle can be used to identify the dominant defect that controls the domain wall formations.

Single file motion (SFM) implies particle motion along quasi one-dimensional (1D) narrow channels where the particles cannot cross each other due to hardcore repulsion. This was originally introduced by Hodgkin and Keynes [1] to describe ion transport in biological channels. Unidirectional or driven SFM have received increasing attention in the recent past for their wide-ranging interdisciplinary applications. We are interested in the role of bottlenecks and their interplay and competition in controlling the stationary states of driven SFM, a question of potential relevance in wide-ranging systems, e.g., traffic flow [2–4] and colloidal particles flowing through geometric constraints [5–7].

Totally asymmetric simple exclusion process (TASEP) serves as a paradigmatic example of 1D driven SFM. Consisting of 1D lattice with L sites, each site of a TASEP can accommodate at most one particle that can hop unidirectionally if the neighbouring site is empty. It was originally proposed to describe protein synthesis by ribosome translocation along messenger RNA strands in eukaryotic cells [8]. Subsequently, it was re-investigated as a simple model for nonequilibrium phase transition in 1D open systems [9, 10].

In this Letter, we study a particle number conserving TASEP in a ring with one point (PD) and one extended (ED) defects as a conceptual model for competition among road blocks in driven SFM having a fixed number of mobile agents. We elucidate how the stationary density profiles of the TASEP emerge as an interplay between the dominant defect and number conservation. Our principal results are (i) at a qualitative level, the defects lead to domain walls (DW) in the stationary density profiles connecting segments lower and higher than

$1/2$, when the system is neither nearly empty or nearly full, but rather has a moderate density. This defines a DW phase. In a striking display of defect competition, the DW location jumps *discontinuously* as the system undergoes a *first order* transition between PD and ED controlled states. (ii) In the DW phase, generally there is a single localised DW (LDW) for both PD or ED. Nonetheless, the LDW profiles for a PD and ED are fundamentally different from each other. (iii) In the event, the two defects are equi-dominant (in the sense explained below), instead of a single LDW, a pair of delocalised domain walls (DDW) emerges, forming *outside* ED. (iv) For a nearly empty or filled system, the density everywhere is less or more than $1/2$, reminiscent of the low density (LD) or high density (HD) phases of a TASEP with open boundary conditions [9–11].

Our results on DWs can be reconciled within a minimum current principle. This study should be useful to understand the phenomenologies of ribosome translocations along closed mRNA loops (circular translation of polysomal mRNA) with clusters of slow codons along which ribosome translocations are inhibited [12–17].

Our model, a periodic TASEP, has a single slow site (PD) at $i = 1$ and an extended slow section (ED) from $i = \epsilon_1 L$ to $(\epsilon_1 + \epsilon_2)L$, $\epsilon_1, \epsilon_2 < 1$; see Fig. 1 for a schematic diagram of the model. The hopping rate across PD is $p < 1$, and ED has a hopping rate $q < 1$. In general $p \neq q$. Elsewhere in the system, the hopping rate is unity. The particles are assumed to move in the anticlockwise direction. It has a mean particle number density n , a constant of motion. The phases in the model and the associated transitions are controlled by p, q, n . The corresponding mean-field phase diagram with $\epsilon_1 = \epsilon_2 = 1/3$ is shown in Fig. 2, giving the phases in the three segments - T_1 between $i = 1$ to $\epsilon_1 L$, T_2 between $\epsilon_1 L$ to $(\epsilon_1 + \epsilon_2)L$ and T_3 between $(\epsilon_1 + \epsilon_2)L$ to L , connected serially. Thus, as n rises from a very low value, the system moves from the LD-LD-LD phase to DW phases, dominated either by PD or ED, or both equally competing, for moderate n ,

*Electronic address: goswami.atri@gmail.com

†Electronic address: rohn.ch@gmail.com

‡Electronic address: sudip.bat@gmail.com, aca.sudip@gmail.com

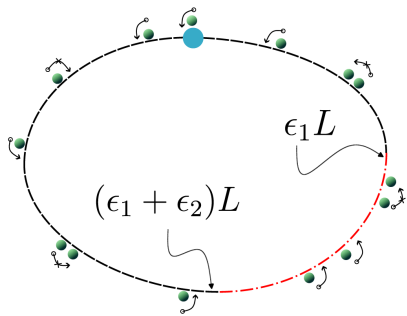


FIG. 1: Schematic model diagram. The thick bluish green circle marks the point defect across which the hopping rate is $p < 1$. The arc in red is the extended defect along which the hopping rate is $q < 1$. In the remaining segments, the hopping rate is unity (see text).

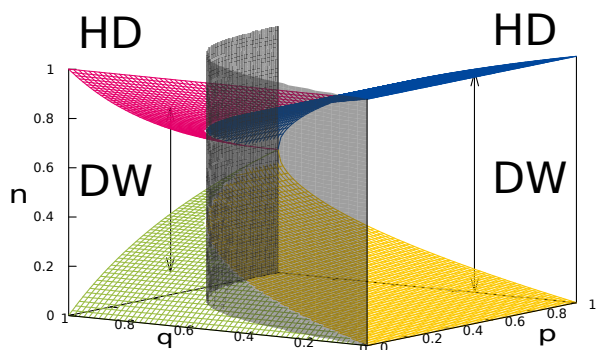


FIG. 2: Mean-field phase diagram of the model in the p - q - n space showing the phases in the model. HD and DW (with one LDW) phases are marked. LD phase that lies below the DW phase in the figure is not visible. Points on the gray curved plane lying as a divider of the DW phase have $J_{PD} = J_{ED}$ satisfied, where J_{PD} , J_{ED} are the steady state currents in the PD and ED dominated situations respectively (see text below) and have a pair of DDWs fully or partially covering T_1 and T_3 . In the DW phase region, on the left of this curved surface (i.e., with $J_{PD} < J_{ED}$, there is an LDW due to the point defect in either T_1, T_2 or T_3 ; on the right of this plane (i.e., with $J_{ED} < J_{PD}$, one has an LDW due to the extended defect in T_1 or T_3 and correspondingly an MC phase in T_2). In the HD (LD) phase region, one has HD-HD-HD (LD-LD-LD) phase in T_1, T_2, T_3 (see text).

eventually to the HD-HD-HD phase for very high n close to unity. These qualitative descriptions are presented in Movies 1, 2, 3 in the Supplemental Material (SM) [18].

Below we derive the results on DWs within a mean-field theory (MFT) [19], supplemented by extensive Monte-Carlo simulations (MCS) studies, providing quantitative basis to the movies in SM. It is convenient to introduce a quasi-continuous coordinate $x \equiv i/L$ in the thermodynamic limit $L \rightarrow \infty$, with $0 \leq x \leq 1$. Now defining $\rho_a(x) \equiv \langle \rho_i^a \rangle$ as the local density, where $\langle \dots \rangle$ implies temporal averages in the steady states and $a = 1, 2$ or 3 for the three segments, the stationary cur-

rents J_1, J_2, J_3 in the three segments in MFT are

$$J_1 = \rho_1(1 - \rho_1), J_2 = q\rho_2(1 - \rho_2), J_3 = \rho_3(1 - \rho_3), \quad (1)$$

where ρ_1, ρ_2 and ρ_3 are the stationary densities in T_1, T_2 and T_3 respectively, are all equal due to current conservation. Particle number conservation (PNC) gives $\int_0^{\epsilon_1} \rho_1 dx + \int_{\epsilon_1}^{\epsilon_1 + \epsilon_2} \rho_2 dx + \int_{\epsilon_1 + \epsilon_2}^1 \rho_3 dx = n$, where $n = \sum_i n_i/L$ is the mean particle density in the system. Steady state currents (1) together with PNC can be used to calculate the steady state densities ρ_1, ρ_2, ρ_3 . A complete characterisation of the steady states of this model requires specifying the phases in all of T_1, T_2, T_3 , i.e., solving for all of ρ_1, ρ_2, ρ_3 . While an open TASEP can be in LD, HD and maximal current (MC) phases, a TASEP in a closed system can also be in domain wall (DW) phase in an extended region of the control parameter space [20–26]. We will see below that current conservation and PNC jointly ensure that *not all* of the possible phases are actually admissible in the present model.

The emergence of DWs, as revealed in our MCS results and observed in the movies [18] can happen in two distinct ways. Physically, from the LD-LD-LD phase upon addition of particles, n rises and it eventually reaches a lower threshold, a macroscopically nonuniform steady state in the shape of a DW is formed. A DW, essentially a pile up of particles due to a bottleneck or a defect, should form *behind* the defect, point or extended, as the case may be, and then start to grow as n rises further. While this remains true independent of the defect, our MCS results reveal a striking aspect - a DW that forms behind a PD can be anywhere in the TASEP ring covering all of T_1, T_2, T_3 , being controlled by n , whereas a DW, which forms behind an ED, never enters T_2 ! This leads to complex density profiles when the two defects are “competing”; see below and also Movie 3 in SM [18]. To proceed systematically, setting aside for the time being the question of which of the two defects will have a DW behind it, let us separately consider DW formations by PD and ED. Considering a PD, a DW is first formed in T_1 , as n just exceeds n_{cL}^p , a threshold for DW formation (see below) with the DW position x_w being at $x = 0$. As n exceeds n_{cL}^p , the size of this pile or the DW increases by shifting its position x_w (see below for a formal definition) along the ring, moving from T_1 first to T_2 and then to T_3 , finally reaching $x = 1$, at which point the DW ends at a threshold n_{cU}^p of n (see below), bringing the model to its HD-HD-HD phase. Now assume a DW at x_w in T_1 , i.e., $0 < x_w < \epsilon_1$, connecting a high density segment with density $\rho_{HD} = 1/(1+p)$ between 0 and x_w and a low density segment with density $\rho_{LD} = p/(1+p)$ between x_w and ϵ_1 [20, 21]. Then using PNC

$$\begin{aligned} \rho_2 &= \left[\frac{1}{2} \pm \left\{ \frac{1}{4} - \frac{p}{q(1+p)^2} \right\}^{1/2} \right] \\ &= \rho_{2+} (> 1/2), \rho_{2-} (< 1/2). \end{aligned} \quad (2)$$

Clearly, these solutions are physically acceptable, so long as $4p/[q(1+p)^2] < 1$. For a DW in T_1 , $\rho_2 = \rho_{2-}$. Then

applying PNC

$$x_w = \left(\frac{1+p}{1-p} \right) [n - \rho_{2-} \epsilon_2 - \rho_{LD}(1 - \epsilon_2)]. \quad (3)$$

Since a unique solution for x_w can be obtained from (3), the DW has a fixed position and hence is an LDW. For $x_w > 0$ but $< \epsilon_1$, there is an LDW in the bulk of T_1 , making ρ_1 nonuniform, corresponding to the DW-LD-LD phase. If we set $x_w = 0$, all of T_1 , T_2 and T_3 are in their LD phases, and is in fact the boundary between the LD-LD-LD phase and DW-LD-LD phase. We get

$$\frac{p}{1+p}(1 - \epsilon_2) + \frac{\epsilon_2}{2} \left[1 - \sqrt{1 - \frac{4p}{q(1+p)^2}} \right] = n_{cL}^p, \quad (4)$$

a lower threshold on n , such that as n exceeds n_{cL}^p a DW due to PD forms in T_1 with the disappearance of the LD-LD-LD phase. As n rises, the LDW shifts first to T_2 and then to T_3 . The corresponding locations can be found by using PNC in a way analogous to the above. In particular, an LDW in T_3 has a location

$$x_w = \left(\frac{1+p}{1-p} \right) \left[n + \epsilon_2 \rho_{HD} - \rho_{LD} - \frac{\epsilon_2}{2} \rho_{2+} \right]. \quad (5)$$

An LDW can be formed in T_2 also; see SM [18] for the corresponding LDW position. At $x_w = 1$, the LDW ends, giving the boundary between the HD-HD-DW and HD-HD-HD phases. We find

$$\frac{\epsilon_1}{1+p} + \frac{\epsilon_2}{2} \left[1 + \sqrt{1 - \frac{4p}{q(1+p)^2}} \right] + \frac{1 - \epsilon_1 - \epsilon_2}{1+p} = n_{cU}^p, \quad (6)$$

an upper threshold on n , such that as n exceeds n_{cU}^p , HD-HD-HD phase reappears. See SM [18] for a similar expression of x_w in T_2 . In fact, an LDW in T_2 assumes a staircase-like shape. See Fig. 3 (left) for a plot of an LDW in T_2 .

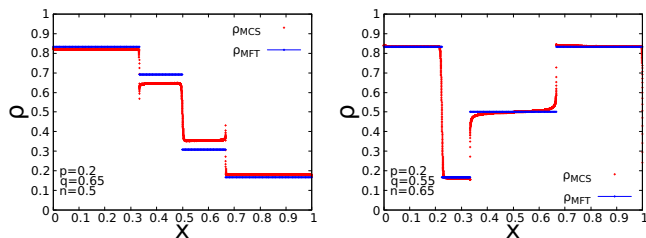


FIG. 3: Plots of LDW due to (left) PD in T_2 with $p = 0.2$, $n = 0.5$, $q = 0.65$, $L = 9000$, $\epsilon_1 = \epsilon_2 = 1/3$, (right) ED in T_1 with $p = 0.2$, $n = 0.65$, $q = 0.55$, $L = 9000$, $\epsilon_1 = \epsilon_2 = 1/3$. MFT (blue lines) and MCS (red points) results are shown (see text).

A DW can however also form behind ED, once a rising n exceeds a *different* lower threshold, denoted n_{cL}^q below. At $n = n_{cL}^q$, T_2 reaches its MC phase with $\rho_2 = 1/2$ in the bulk, and $\rho_1 = \rho_3 < 1/2$. As n is further increased

beyond n_{cL}^q , a DW is formed in the system, just behind the bottleneck. In the ED dominated regime considered here, T_2 is the (extended) bottleneck. This means a DW is first formed at $x = \epsilon_1 + \epsilon_2$ in T_3 as soon as n reaches n_{cL}^q . As n rises further, the DW starts moving along T_3 , crossing over to T_1 at $x = 0$, and then finally reaching $x = \epsilon_1$ at an upper density threshold n_{cU}^q , when the DW ends. Any further increase in n will push the system to the HD-HD-HD phase. Thus, the DW *never enters* T_2 , which remains in its MC phase. This is a fundamental difference with the LDW formed due to PD.

With T_2 in its MC phase, $\rho_2 = 1/2$ and $J_2 = q/4$. Current conservation then yields (ρ being ρ_1 or ρ_3)

$$\rho = \frac{1}{2} \left[1 \pm \sqrt{1 - q} \right] = \rho_+ (> 1/2), \rho_- (< 1/2), \quad (7)$$

giving the densities of the high density and low density parts of the DW, which meet at x_w . Using the logic outlined above for a PD together with (7) and PNC, we find with $x_w = \epsilon_1 + \epsilon_2$

$$(1 - \epsilon_2) \frac{1}{2} \left[1 - \sqrt{1 - q} \right] + \frac{\epsilon_2}{2} = n \equiv n_{cL}^q, \quad (8)$$

a critical density above which an LDW due to ED appears that sets the beginning of LD-MC-DW phase. Likewise, assuming an LDW in T_1 and setting $x_w = \epsilon_1$ gives

$$(1 - \epsilon_2) \frac{1}{2} \left[1 + \sqrt{1 - q} \right] + \frac{\epsilon_2}{2} = n \equiv n_{cU}^q, \quad (9)$$

defining an upper threshold on n , such that for $n > n_{cU}^q$, HD-HD-HD phase ensues. Our MFT and MCS results on LDW in T_1 is shown in Fig. 3 (right). Following the logic outlined above the LDW position in T_1 or T_3 due to ED can be found straightforwardly [18].

A minimum current principle determines which of the two possible routes to DW formations is actually realised for a given (p, q) . The stationary current J_{PD} corresponding to a domain wall solution due to PD is $J_{PD} = p/(1+p)^2$. Similarly, the stationary current J_{ED} corresponding to a domain wall due to ED is $J_{ED} = q/4$. Minimum current principle stipulates that when $J_{PD} < (>) J_{ED}$, the nonuniform steady states are controlled by the PD (ED), which is consistent with our MCS results. When $J_{PD} = J_{ED}$, the two defects compete, as we illustrate below, a new kind of states - a pair of delocalised domain walls (DDW) emerges as long as n exceeds both n_{cL}^q , n_{cL}^p , but less than n_{cU}^q , n_{cU}^p . Following the logic of LDW formation in PD and ED dominated regimes, we then expect one DW, say at $x = x_w^{ED}$, due to ED, and another, $x = x_w^{PD}$, due to PD. Thus, a complete description of the stationary density profiles require enumeration of both x_w^{PD} and x_w^{ED} . However, with just one condition, *viz.*, the PNC at hand, both x_w^{PD} and x_w^{ED} cannot be uniquely determined. Rather a linear relation between the two is obtained. This means any pair of (x_w^{PD}, x_w^{ED}) satisfying PNC is a valid solution. Since a DW due to ED must be confined to T_1 and T_3 only

(see above), other DW due to PD must also be confined to the same (even though an LDW due to an isolated PD with $J_{PD} < J_{ED}$ can also be in T_2). Thus, each of (x_w^{PD}, x_w^{ED}) must be confined to T_1 or T_3 only. The inherent stochasticity of the dynamics implies all such (x_w^{PD}, x_w^{ED}) pairs satisfying PNC are visited over time. This further means long-time averages of the densities are *inclined* straight lines. As a concrete example, assume $n_{cL}^p, n_{cL}^q < n < 1/2$ together with $J_{ED} = J_{PD}$. Both the DWs must have the same height $(1-p)/(1+p)$, with $\rho_{HD} = 1/(1+p)$, $\rho_{LD} = p/(1+p)$, $\rho_2 = 1/2$. Applying PNC,

$$\begin{aligned} \rho_{HD} x_w^{PD} + \rho_{LD} (\epsilon_1 - x_w^{PD}) + \frac{\epsilon_2}{2} + \frac{x_w^{ED} - \epsilon_1 - \epsilon_2}{1+p} \\ + \frac{p(1-x_w^{ED})}{1+p} = n, \end{aligned} \quad (10)$$

giving a linear relation connecting x_w^{PD} and x_w^{ED} , and not each of the positions separately. As a result, a pair of DDWs is observed. MFT cannot predict the profiles of the DDWs, as it neglects fluctuations. However, we can employ arguments based on symmetry to construct the DDW profiles. Focussing on the case $\epsilon_1 = 1/3 = \epsilon_2$ and exploiting the statistical equivalence of the configurations of the long time averaged envelop of the DDWs in T_1 and T_3 , we hypothetically replace each of them by an LDW of height $(1-p)/(1+p)$, connecting $\rho_{HD} = 1/(1+p)$ and $\rho_{LD} = p/(1+p)$. Such (hypothetical) replacements evidently satisfy the PNC. Symmetry of the problem dictates that if x_0 is the position of the LDW in T_1 , the corresponding LDW in T_3 must be located at $x_0 + 2/3$. Application of PNC then gives

$$2x_0 \frac{1-p}{1+p} = n - \frac{1}{6} - \frac{2}{3} \left(\frac{p}{1+p} \right). \quad (11)$$

Clearly, if $n = 1/2$, $x_0 = 1/6$, which means the midpoint of the LDW is at the midpoint of T_1 or T_3 , corresponding to DDWs covering entire T_1 and T_3 . If $n < 1/2$, $x_0 < 1/6$, whereas $n > 1/2$, $x_0 > 1/6$, both of which correspond to DDWs partially covering T_1 and T_3 . With the knowledge of x_0 , it is now possible to obtain the DDW envelop. For instance with $n < 1/2$, there is an LD segment in the DDWs in both T_1 and T_3 , which are of length $1/3 - 2x_0$. In other words, the DDW in T_1 (T_3) wanders a distance $2x_0$, starting from $x = 0$ ($x = \epsilon_1 + \epsilon_2$). Then joining the densities at $x = 0, 2x_0$ ($x = \epsilon_1 + \epsilon_2, \epsilon_1 + \epsilon_2 + 2x_0$) gives the profiles of the DDW in T_1 (T_2). Our MCS results on DDWs in T_1, T_3 and the corresponding kymographs are shown in Fig. 4. The analytically obtained DDW profiles are also shown. The kymographs clearly show the synchronised nature of the DDW movements fully or partially covering T_1 and T_3 . See [18] for a related movie (Movie 4) that visually presents this picture, showing a pair of DDWs, partial or full as controlled by n .

Since a DW due to PD *can* be inside T_2 , whereas a DW due to ED *cannot* be, an intriguing situation can arise when an LDW due to PD is formed in T_2 , with $J_{PD} <$

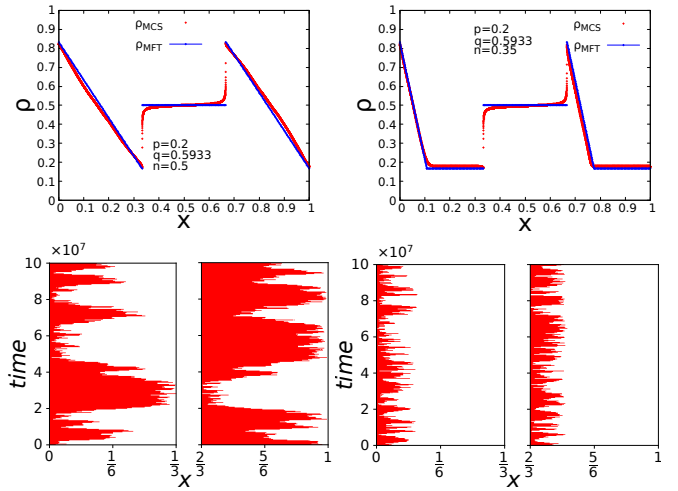


FIG. 4: Plot of a pair of DDWs in T_1 and T_3 with (top left) $n = 0.5$, $p = 0.2$, $q = 0.5933$, $L = 9000$, $\epsilon_1 = \epsilon_2 = 1/3$, (top right) $n = 0.35$, $p = 0.2$, $q = 0.5933$, $L = 9000$, $\epsilon_1 = \epsilon_2 = 1/3$, and corresponding kymographs (bottom left) and (bottom right). The analytically obtained DDW profiles (blue lines) and MCS results (red points) are shown (see text).

J_{ED} *only slightly*. By tuning (p, q) , one can make $J_{PD} > J_{ED}$ again *only slightly*, for which an LDW is formed due to ED, which however cannot be in T_2 ! Thus the LDW position can jump *discontinuously* under a small change in the defect strengths; see movies 5 and 6 in SM [18]. As an example, consider $n = 1/2$ and p_c, q_c satisfy $J_{PD} = J_{ED}$ together with $\epsilon_1 = \epsilon_2 = 1/3$. Then if $p = p_c - \delta_1$, $q = q_c + \delta_2$, $\delta_1, \delta_2 > 0$ (but δ_1, δ_2 are very small) $J_{PD} < J_{ED}$, we have an LDW at $x_w = 1/2$ due to the point defect [18]. On the other hand, if $\delta_1, \delta_2 < 0$, $J_{ED} < J_{PD}$ and hence an LDW at $x_w = 0$. Thus, as one moves $\mathcal{O}(\delta)$, $\delta = \delta_1, \delta_2$ being vanishingly small, the DW position changes by an $\mathcal{O}(1)$ amount - from $x_w = 0$ to $x_w = 1/2$. Thus x_w as a function of δ_1, δ_2 (or p, q) shows a jump across the line $J_{PD} = J_{ED}$: let $\delta \equiv 2\sqrt{\delta_1^2 + \delta_2^2}$ be the “distance” between the two points $(p = p_c - \delta_1, q = q_c + \delta_2)$ and $(p = p_c + \delta_1, q = q_c - \delta_2)$ in the $p-q$ plane. Then, $dx_w/d\delta$ diverges for small δ . Such divergences, a hallmark of defect competition, can occur only when the two points in the $p-q$ plane lie on the two sides of the line determined by the condition $J_{PD} = J_{ED}$. This jump in x_w across the line $J_{PD} = J_{ED}$ indicates a discontinuous transition between the PD and ED dominated steady states each with one LDW, with x_w appearing as an order parameter.

The density profiles in LD-LD-LD and HD-HD-HD phases are straightforward to obtain by using PNC and current conservation; see SM [18]. Phase boundaries (4), (6), (8) and (9) give the phase diagram in Fig. (2).

In summary, we have developed a theory for bottleneck competition in closed, driven SFM by studying a conceptual model consisting of a TASEP with a PD and an ED in a ring geometry. This reveals how a dominant defect enforces a particular form of LDW, when sufficient number of particles are available. When they are competing,

a pair of DDWs are obtained, instead of a single LDW. We show how the competition between the defects manifests strikingly in the discontinuous jump of the LDW location, as the system passes from being controlled by one defect to another. Our theory can be generalised to arbitrary number of PD or ED straightforwardly. Our results can be experimentally studied in model experiments on the collective motion of driven particles with light-induced activity [27] through a closed narrow circular channel [28, 29]. Suppression of rotational diffusion,

e.g., by choosing ellipsoidal particles with the channel width shorter than the long axis of the particle everywhere, or by using dimer particles can enforce unidirectional movements. Lastly, in spite of the simplicity of our model, the results from it should give insight about the effects of bottlenecks on directional motion in more complex living [2–4] or *in-vitro* [5–7] systems.

Acknowledgement:- S.M. thanks SERB (DST), India for partial financial support through the CRG scheme [file: CRG/2021/001875].

-
- [1] A. L. Hodgkin and R. D. Keynes, The potassium permeability of a giant nerve fibre, *J. Physiol.* **128**, 61 (1955).
- [2] V. Ziemer, A. Seyfried and A. Schadschneider, Congestion Dynamics in Pedestrian Single-File Motion, arXiv:1602.03053.
- [3] D. Chowdhury, L. Santen and A. Schadschneider, Statistical physics of vehicular traffic and some related systems, *Phys. Rep.* **329**, 199 (2000).
- [4] D. Helbing, Traffic and related self-driven many-particle systems, *Rev. Mod. Phys.* **73**, 1067 (2001).
- [5] A. Janda, I. Zuriguel, & D. Maza, Flow rate of particles through apertures obtained from self-similar density and velocity profiles. *Phys. Rev. Lett.* **108**, 248001 (2012).
- [6] M. Souzy, I. Zuriguel, & A. Marin, Transition from clogging to continuous flow in constricted particle suspensions. *Phys. Rev. E* **101**, 060901 (2020).
- [7] S. G. Leyva, R. L. Stoop, P. Tierno, & I. Pagonabarraga, Dynamics and clogging of colloidal monolayers magnetically driven through a heterogeneous landscape. *Soft Matter* **16**, 6985 (2020).
- [8] J. MacDonald, J. Gibbs and A. Pipkin, Kinetics of biopolymerization on nucleic acid templates, *Biopolymers* **6**, 1 (1968).
- [9] J. Krug, Boundary-induced phase transitions in driven diffusive systems, *Phys. Rev. Lett.* **67**, 1882 (1991).
- [10] T Chou, K Mallick, and R K P Zia, Non-equilibrium statistical mechanics: From a paradigmatic model to biological transport, *Rep. Prog. Phys.* **74**, 116601 (2011).
- [11] B. Schmittmann and R. Zia, in *Phase Transitions and Critical Phenomena*, edited by C. Domb and J. L. Lebowitz (Academic, London, 1995).
- [12] T. Chou, Ribosome Recycling, Diffusion, and mRNA Loop Formation in Translational Regulation, *Biophys. J.* **85**, 755 (2003).
- [13] S. E. Wells, E. Hillner, R. D. Vale and A. B. Sachs, Circularization of mRNA by Eukaryotic Translation Initiation Factors, *Mol. Cell* **2**, 135 (1998).
- [14] G. S. Kopeina et al, Step-wise formation of eukaryotic double-row polyribosomes and circular translation of polysomal mRNA, *Nucleic Acids Res.* **36**, 2476 (2008).
- [15] Robinson M et al, Codon usage can affect efficiency of translation of genes in *Escherichia coli*, *Nucleic Acids Res.* **12**, 6663 (1984).
- [16] M. A. Sorensen, C. G. Kurland and S. Pedersen, Codon usage determines translation rate in *Escherichia coli*, *J. Mol. Biol.* **207**, 365 (1989).
- [17] D. A. Phoenix and E. Korotkov, Evidence of rare codon clusters within *Escherichia coli* coding regions, *FEMS Microbiol. Lett.* **155**, 63 (1997).
- [18] See Supplemental Material (SM) for Movies 1, 2, 3, 4, 5 and 6, and results on the LD-LD-LD/HD-HD-HD phases and additional details on LDWs.
- [19] R. A. Blythe and M. R. Evans, Nonequilibrium steady states of matrix-product form: a solver's guide, *J. Phys. A* **40**, R333 (2007).
- [20] S. A. Janowsky and J. L. Lebowitz, Finite-size effects and shock fluctuations in the asymmetric simple-exclusion process, *Phys. Rev. A* **45**, 618 (1992).
- [21] N. Sarkar and A. Basu, Nonequilibrium steady states in asymmetric exclusion processes on a ring with bottlenecks, *Phys. Rev. E* **90**, 022109 (2014).
- [22] G. Tripathy and M. Barma, Driven lattice gases with quenched disorder: Exact results and different macroscopic regimes, *Phys. Rev. E* **58**, 1911 (1998).
- [23] H. Hinsch and E. Frey, Bulk-driven nonequilibrium phase transitions in a mesoscopic ring, *Phys. Rev. Lett.* **97**, 095701 (2006).
- [24] T. Banerjee, N. Sarkar and A. Basu, Generic nonequilibrium steady states in an exclusion process on an inhomogeneous ring, *J. Stat. Mech. J. Stat. Mech.* P01024 (2015).
- [25] P. Roy, A. K. Chandra and A. Basu, Pinned or moving: States of a single shock in a ring, *Phys. Rev. E* **102**, 012105 (2020).
- [26] A. Haldar, P. Roy and A. Basu, Asymmetric exclusion processes with fixed resources: Reservoir crowding and steady states, *Phys. Rev. E* **104**, 034106 (2021).
- [27] I. Buttinoni et al, Active Brownian motion tunable by light, *J. Phys. Condens. Matter* **24**, 284129 (2012).
- [28] Q.-H. Wei, C. Bechinger, and P. Leiderer, Single-File Diffusion of Colloids in One-Dimensional Channels, *Science* **287**, 625 (2000).
- [29] C. Bechinger et al, Active Particles in Complex and Crowded Environments, *Rev. Mod. Phys.* **88**, 045006 (2016).

Supplemental Material

Defect versus defect: stationary states of single file marching in periodic landscapes with road blocks

I. MEAN-FIELD THEORY FOR THE STATIONARY DENSITY PROFILES

In this Section, we set up and analyze the MFT equations [1]. Let n_i be the occupation at site i . In the MFT approximation, correlations are neglected and averages of products are replaced by products of averages [19]. While MFT is an adhoc approximation, it provides a good analytically tractable guideline to the steady state densities and phase diagrams. It is convenient to consider the system to be composed of three segments - T_1 between $i = 1$ to $\epsilon_1 L$, T_2 between $\epsilon_1 L$ to $(\epsilon_1 + \epsilon_2)L$ and T_3 between $(\epsilon_1 + \epsilon_2)L$ to L , connected serially. The MFT equation for the density n_i in the different segments reads

$$\frac{dn_i}{dt} = n_{i+1}[1 - n_i] - n_i[1 - n_{i-1}], \quad 1 < i < \epsilon_1 L, \quad (12)$$

$$= qn_{i+1}[1 - n_i] - qn_i[1 - n_{i-1}], \quad (13)$$

$$\epsilon_1 L \leq i \leq (\epsilon_1 + \epsilon_2)L, \quad (13)$$

$$= n_{i+1}[1 - n_i] - n_i[1 - n_{i-1}], \quad (14)$$

$$(\epsilon_1 + \epsilon_2)L < i \leq L. \quad (14)$$

We note that the above mean-field equations are invariant under the transformations $n_i \rightarrow 1 - n_{L-i-1}$, which defines the particle hole symmetry in this model. Before proceeding further it is convenient to introduce a quasi-continuous coordinate $x \equiv i/L$ in the thermodynamic limit $L \rightarrow \infty$. Thus, we have $0 \leq x \leq 1$. Now define $\rho_a(x) \equiv \langle n_i^a \rangle$, where $\langle \dots \rangle$ implies temporal averages in the steady states and $a = 1, 2$ or 3 for the three segments.

We recall, as given the main text, that the stationary currents J_1, J_2, J_3 in the three segments in MFT

$$J_1 = \rho_1(1 - \rho_1), \quad (15)$$

$$J_2 = q\rho_2(1 - \rho_2), \quad (16)$$

$$J_3 = \rho_3(1 - \rho_3), \quad (17)$$

where ρ_1, ρ_2 and ρ_3 are the stationary densities in T_1, T_2 and T_3 respectively, are all equal due to current conservation:

$$J_1 = J_2 = J_3 \quad (18)$$

in the steady states.

A. LD-LD-LD phase

For sufficiently low mean densities n , all the channels should be sparsely populated, and hence we expect all the three segments to be in their LD phases with uniform densities $\rho_1 = \rho_3 < \rho_2 < 1/2$ respectively. These may be obtained as follows. By using $J_1 = J_2 = J_3$

$$\rho_1(1 - \rho_1) = q\rho_2(1 - \rho_2) = \rho_3(1 - \rho_3). \quad (19)$$

Now using particle number conservation, we get

$$[1 - \epsilon_2]\rho_1 + \rho_2\epsilon_2 = n. \quad (20)$$

For explicit solutions of the densities, (19) together with (20) can be used to give

$$\rho_1 = \left[-B \pm \sqrt{B^2 - 4AC} \right] \frac{1}{2A}, \quad (21)$$

as the two general solutions, where

$$A = (1 - \epsilon_2)^2 - \epsilon_2^2/q, \quad (22)$$

$$B = \frac{\epsilon_2^2}{q} - (1 - \epsilon_2)(2n - \epsilon_2), \quad (23)$$

$$C = n^2 - \epsilon_2 n. \quad (24)$$

So far we have not imposed any conditions of the LD-LD-LD phase on the solutions (21). The pertinent question then is: Which of the two solutions in (21) is to be considered as the LD-LD-LD phase density solution? To settle this, we use the fact that in the limiting case with vanishing particle number, i.e., with $n \rightarrow 0$, the LD-LD-LD phase solution must smoothly go to zero. This consideration allows us to pick the right solution in (21) for the LD-LD-LD phase: we choose the solution that vanishes as $n \rightarrow 0$. Which one among the two in (21) does that depends upon the signs of A and B , i.e., will be decided by ϵ_2 and n . We thus note that the point defect has no macroscopic effect on the steady state density profiles. Instead at $x = 0$, the location of the point defect, there is a local peak of height h with vanishing width in the thermodynamic limit, where $h = \rho_1(1-p)/p$, such that the local density at $x = 0$ is $\rho_1 + h$ [2, 3]. This essentially acts as a boundary layer between T_1 and T_3 . Steady state density profiles in the LD-LD-LD phase with $n = 0.15, p = 0.2, q = 0.45$ and $n = 0.15, p = 0.15, q = 0.6$ with a system size $L = 9000$ and $\epsilon_1 = \epsilon_2 = 1/3$ are shown in Fig. 5. Good agreement between MFT and MCS results are observed.

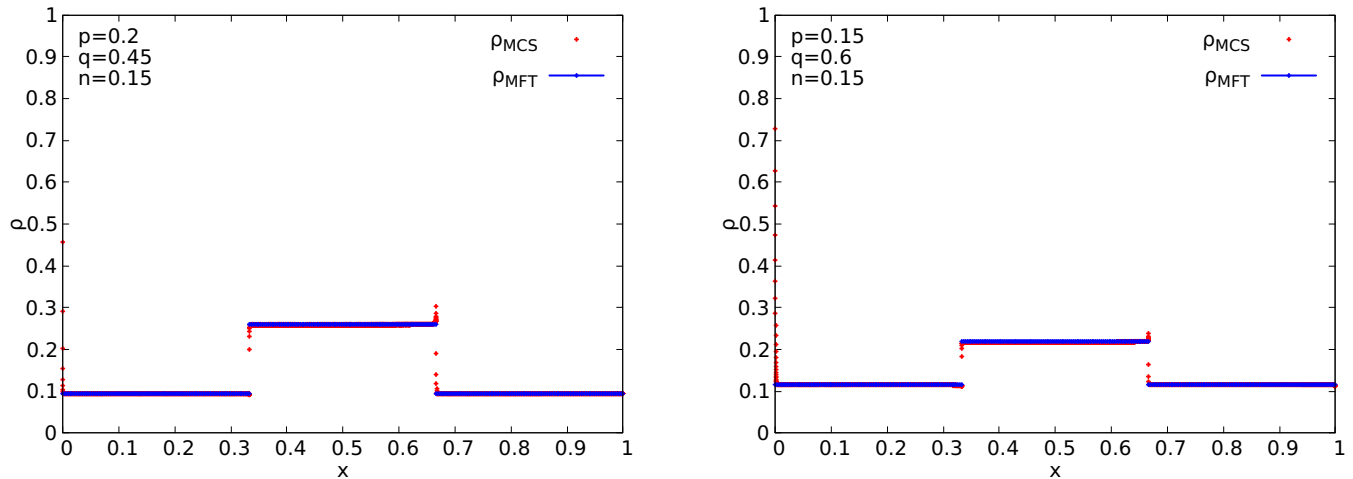


FIG. 5: LD-LD-LD density plots with $n = 0.15$: (left) $p = 0.2, q = 0.45$, (right) $p = 0.15, q = 0.6$. MFT (blue lines) and MCS (red points) results are shown. Good agreement between MFT and MCS results are observed.

B. HD-HD-HD phase

The HD-HD-HD phase can be analysed by applying the particle-hole symmetry on the LD-LD-LD phase. Physically, for very high n , all of T_1, T_2 and T_3 should be nearly filled with particles, and hence HD-HD-HD phase is expected. In this case, $\rho_1, \rho_2, \rho_3 > 1/2$ and $\rho_1 = \rho_3 > \rho_2$.

For an explicit solution for the HD-HD-HD phase, we again consider (21) and note that if $n = 1$, unsurprisingly $\rho_1 = 1$ is a solution, which in turn means $\rho_2 = 1$ and $\rho_3 = 1$, i.e., a completely filled up system. Thus, when the system is nearly filled and all of T_1, T_2, T_3 are in their HD phases, we should accept that particular solution in (21) which smoothly reaches unity when $n \rightarrow 1$. Which of the two solutions in (21) will satisfy this property depends on the signs of A, B .

Similar to the LD-LD-LD phase, the point defect has no macroscopic effect on the stationary densities. Instead, one has a local dip of depth h' , with vanishing width in the thermodynamic limit, where $h' = (1 - \rho_1)(1 - p)/p$, such that at $x = 0$, the density is $\rho_1 - h'$. Steady state density profiles in the HD-HD-HD phase with $n = 0.8, p = 0.2, q = 0.45$ and $n = 0.8, p = 0.15, q = 0.6$ with a system size $L = 9000$ and $\epsilon_1 = \epsilon_2 = 1/3$ are shown in Fig. 6. Good agreement between MFT and MCS results are observed.

C. MC-MC-MC phase

In the MC phase, the density should be $1/2$. This means in these putative MC phases, $J_1 = J_3 = 1/4, J_2 = q/4$. This immediately shows that there is no MC-MC-MC phase in the model, i.e., all the three segments cannot be simultaneously in the MC phases, as that would violate the current conservation condition (19).

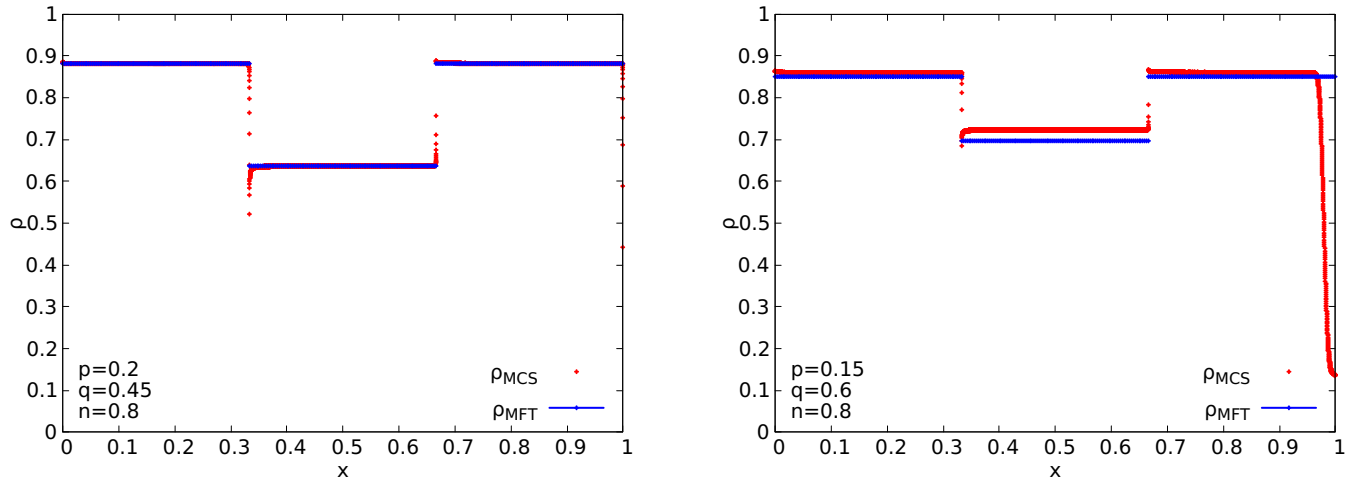


FIG. 6: HD-HD-HD density plots: (left) $n = 0.8$, $p = 0.2$, $q = 0.45$, (right) $n = 0.8$, $p = 0.15$, $q = 0.6$. MFT (blue lines) and MCS (red points) results are shown. Good agreement between MFT and MCS results are observed.

II. LDWS DUE TO THE POINT DEFECT

In the main text, we have presented a plot of LDW in T_2 due to the point defect, giving a staircase-like stationary density profile, as obtained from our MFT and MCS studies. As mentioned in the main text, an LDW due to a point defect can be *anywhere* in the ring, i.e., it can be in T_1 and T_3 as well.

First consider the case when the LDW is inside T_1 : $0 \leq x_w \leq \epsilon_1$. Since the particles flow in the anticlockwise direction, and an LDW should form *behind* a bottleneck (which in the present case is the point defect at $x = 0$), we write

$$\begin{aligned} \rho_1(x) &= \rho_{\text{HD}}, \quad 0 \leq x \leq x_w, \\ &= \rho_{\text{LD}}, \quad x_w \leq x \leq \epsilon_1, \end{aligned} \quad (25)$$

In this situation, we must have the entire T_2 to be its LD phase: $\rho_2(x) = \rho_{2-}$ for $\epsilon_1 \leq x \leq \epsilon_1 + \epsilon_2$. In addition, T_3 too should be in its LD phase, with $\rho_3 = \rho_{\text{LD}}$. We can now apply PNC to determine x_w . We get

$$\rho_{\text{HD}}x_w + \rho_{\text{LD}}(\epsilon_1 - x_w) + \rho_{2-}\epsilon_2 + \rho_{\text{LD}}(1 - \epsilon_1 - \epsilon_2) = n. \quad (26)$$

Equation (26) gives x_w as a function of p , q and n . Simplifying (26), we obtain

$$x_w = \left(\frac{1+p}{1-p} \right) [n - \rho_{2-}\epsilon_2 - \rho_{\text{LD}}(1 - \epsilon_2)], \quad (27)$$

giving a unique solution for x_w , as it should be for an LDW. For $x_w > 0$ but $< \epsilon_1$, there is an LDW in the bulk of T_1 , making ρ_1 nonuniform, corresponding to the DW-LD-LD phase.

When the LDW is inside T_2 , T_1 is in its HD phase, hence $\rho_1 = \rho_{\text{HD}}$, and T_3 is in its LD phase, with $\rho_3 = \rho_{\text{LD}}$. Further, since the LDW is located inside T_2 , we must have $\rho_2 = \rho_+$ for $\epsilon_1 < x < x_w$; $\rho_2 = \rho_-$ for $x_w < x < \epsilon_1 + \epsilon_2$. Applying PNC we get

$$\rho_{\text{HD}}\epsilon_1 + (x_w - \epsilon_1)\rho_{2+} + (\epsilon_1 + \epsilon_2 - x_w)\rho_{2-} + \rho_{\text{LD}}(1 - \epsilon_1 - \epsilon_2) = n. \quad (28)$$

Solving (28), we get

$$x_w = \frac{1}{(\rho_{2+} - \rho_{2-})} \left[n + \rho_{2+}\epsilon_1 - \rho_{\text{HD}}\epsilon_1 - (\epsilon_1 + \epsilon_2)\rho_{2-} - \rho_{\text{LD}}(1 - \epsilon_1 - \epsilon_2) \right] \quad (29)$$

giving a unique position of the LDW in T_2 . The overall density profile, consisting of HD phase in T_1 and LD phase in T_3 , with an intervening LDW in T_2 takes the form of a step-like structure. This is specifically attributed to T_2 being an extended defect with a hopping rate $q < 1$. This is shown in Fig. 3 (left) of the main text.

Next, consider an LDW in T_3 . Thus, $\rho_3(x) = \rho_{\text{HD}}$, $\epsilon_1 + \epsilon_2 < x < x_w$, $\rho_3(x) = \rho_{\text{LD}}$, $x_w < x < 1$. Further, $\rho_1(x) = \rho_{\text{HD}}$, $\rho_2(x) = \rho_+$, since both T_1 and T_2 are in their HD phases. Then applying PNC, we obtain

$$\frac{\epsilon_1}{1+p} + \frac{\epsilon_2}{2} \left[1 + \sqrt{1 - \frac{4p}{q(1+p)^2}} \right] + (x_w - \epsilon_1 - \epsilon_2) \frac{1}{1+p} + \frac{(1-x_w)p}{1+p} = n. \quad (30)$$

Solving, we find

$$x_w = \frac{1+p}{1-p} \left[n + \frac{\epsilon_2}{1+p} - \frac{p}{1+p} - \frac{\epsilon_2}{2} \left[1 + \sqrt{1 - \frac{4p}{q(1+p)^2}} \right] \right] \quad (31)$$

as the LDW position in T_3 .

Our MFT and MCS results on LDWs in T_1 , T_3 are shown in Fig. 7 (left) and Fig. 7 (right) respectively. We find reasonable agreement between our MFT and MCS results.

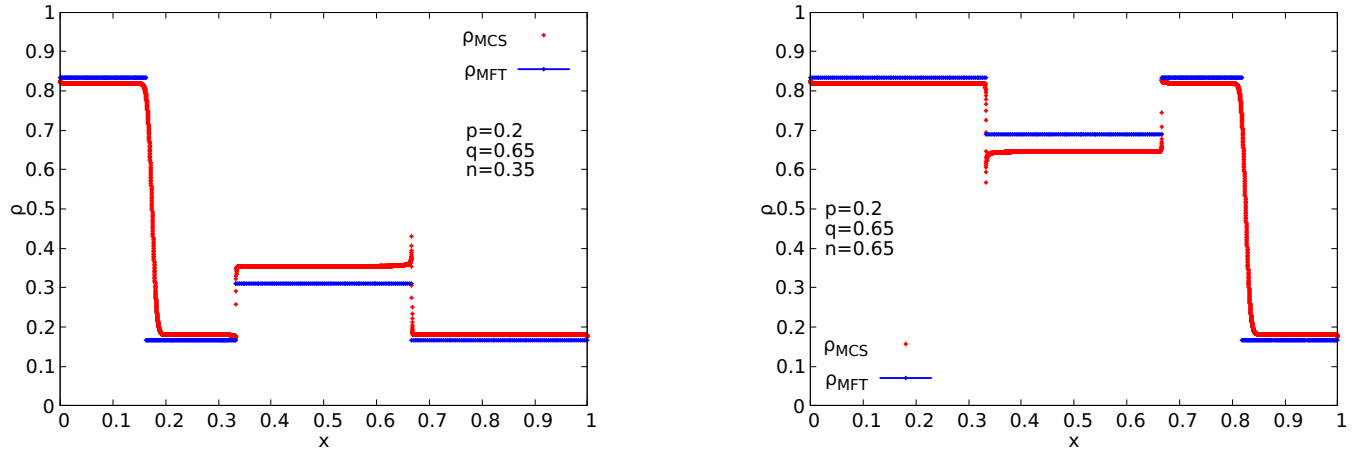


FIG. 7: Plot of an LDW in (left) T_1 in the point defect dominated regime with $p = 0.2, n = 0.35, q = 0.65, L = 9000, \epsilon_1 = \epsilon_2 = 1/3$, and (right) T_3 in the point defect dominated regime with $p = 0.2, n = 0.65, q = 0.65, L = 9000, \epsilon_1 = \epsilon_2 = 1/3$. MFT (blue lines) and MCS (red points) results are shown (see text).

III. LDWS DUE TO THE EXTENDED DEFECT

As mentioned in the main text, an LDW can be formed due to the extended defect as well. In this case, T_2 is in its MC phase with $\rho_2 = 1/2$, and an LDW can be formed in either T_1 or T_3 . In the main text, we have shown an LDW in T_1 due to the extended defect obtained from our MFT and MCS studies. Here, we present an LDW in T_3 due to the extended defect in Fig. 8.

Current conservation yields

$$\rho(1 - \rho) = \frac{q}{4}, \quad (32)$$

where ρ is ρ_1 or ρ_3 . Solving,

$$\rho = \frac{1}{2} \left[1 \pm \sqrt{1 - q} \right] = \rho_+ (> 1/2), \rho_- (< 1/2), \quad (33)$$

giving the densities of the high density and low density parts of the DW, which meet at x_w . As before, x_w can be calculated by using PNC. Assume an LDW in T_3 . This is the LD-MC-DW phase. Then PNC gives

$$\rho_- \epsilon_1 + \frac{\epsilon_2}{2} + (x_w - \epsilon_1 - \epsilon_2) \rho_+ + (1 - x_w) \rho_- = n. \quad (34)$$

Setting $x_w = \epsilon_1 + \epsilon_2$ gives the condition for transition from the LD-LD-LD phase to LD-MC-DW phase, when the DW is due to the extended defect. We get

$$\epsilon_1 \rho_- + \frac{\epsilon_2}{2} + (1 - \epsilon_1 - \epsilon_2) \rho_- = n. \quad (35)$$

This is independent of p , but depends upon q through the dependence of ρ_- on q . Using (33), we find

$$(1 - \epsilon_2) \frac{1}{2} \left[1 - \sqrt{1 - q} \right] + \frac{\epsilon_2}{2} = n \equiv n_{cL}^q, \quad (36)$$

defining a critical density n_{cL}^q above which an LDW due to the extended defect appears.

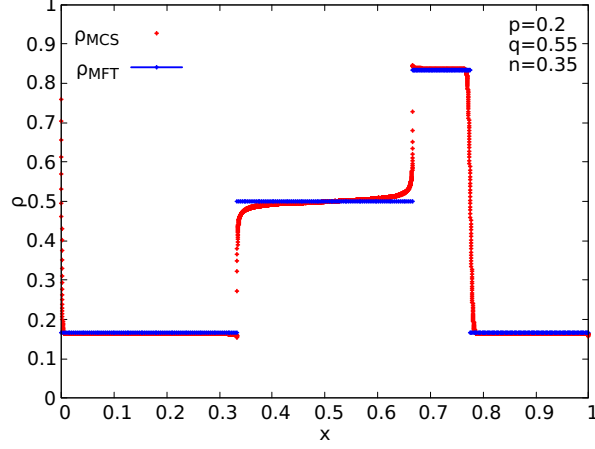


FIG. 8: Plot of an LDW in T_3 in the extended defect dominated regime with $p = 0.2, n = 0.35, q = 0.55, L = 9000, \epsilon_1 = \epsilon_2 = 1/3$. MFT (blue lines) and MCS (red points) results are shown (see text).

Now consider an LDW in T_1 . In this case, T_3 is in the HD phase. PNC gives

$$(\epsilon_1 - x_w)\rho_- + x_w\rho_+ + \frac{\epsilon_2}{2} + (1 - \epsilon_1 - \epsilon_2)\rho_+ = n. \quad (37)$$

Setting $x_w = \epsilon_1$ produces the boundary between the DW-MC-HD phase and HD-HD-HD phase:

$$(1 - \epsilon_2)\rho_+ + \frac{\epsilon_2}{2} = n. \quad (38)$$

Substituting for ρ_+ , we get

$$(1 - \epsilon_2) \frac{1}{2} \left[1 + \sqrt{1 - q} \right] + \frac{\epsilon_2}{2} = n \equiv n_{cU}^q, \quad (39)$$

defining an upper threshold on n , such that for $n > n_{cU}^q$, HD-HD-HD phase is predicted.

-
- [1] R A Blythe and M R Evans, Nonequilibrium steady states of matrix-product form: a solver's guide, J. Phys. A **40**, R333 (2007).
 [2] P. Pierobon, M. Mobilia, R. Kouyos and E. Frey, Bottleneck-induced transitions in a minimal model for intracellular transport, Phys. Rev. E **74**, 031906 (2006).
 [3] N. Sarkar and A. Basu, Nonequilibrium steady states in asymmetric exclusion processes on a ring with bottlenecks, Phys. Rev. E **90**, 022109 (2014).
-